A Deep Neural Network Model of Global Topside Electron Temperature Using Incoherent Scatter Radars and Its Application to GNSS Radio Occultation

Andong Hu[1,2*], Brett Carter[2], Julie Currie[2], Enrico Camporeale[1], Jannis Teunissen[1], Robert Norman[2], Kefei Zhang[2]
[1] Multiscale Dynamic Group, CWI, Amsterdam, Netherlands
[2] SPACE Centre, School of Mathematical and Geospatial Sciences, RMIT University, Melbourne, Australia
***andong@cwi.nl**

Introduction

Ionospheric plasma temperature (Tp) reflects the overall energy absorbed from solar and cosmic radiation by the upper atmosphere and is one of the essential factors reflecting the ionospheric variability. It is also found that the variation of Tp affects the thermal equilibrium in the Earth's upper atmosphere significantly. Tp is taken to be the average of ion temperature Ti and electron temperature Te. The value and variation of Te is considerably larger than those of Ti, especially in the topside ionosphere. Hence, Te variation (in both spatial and temporal domains) is the primary research focus of this study. Obtaining a high-resolution high-quality Te map all over the globe could prove to be significant for gaining a better understanding of the upper atmosphere and its interaction with the space environment.

The goals of this study are:

- To develop a new model for global topside **electron temperature (Te)** using a **deep neural network (DNN)** that is trained using measurements from **Incoherent Scatter Radars (ISRs)**.
- To investigate whether this model can be used to generate the electron temperature in the topside ionosphere using **GNSS ionospheric radio occultation (GNSS-IRO)** data as the input.
- To analyse the diurnal electron temperature profiles obtained from GNSS-IRO in comparison with the TIEGCM outputs.

Methodology

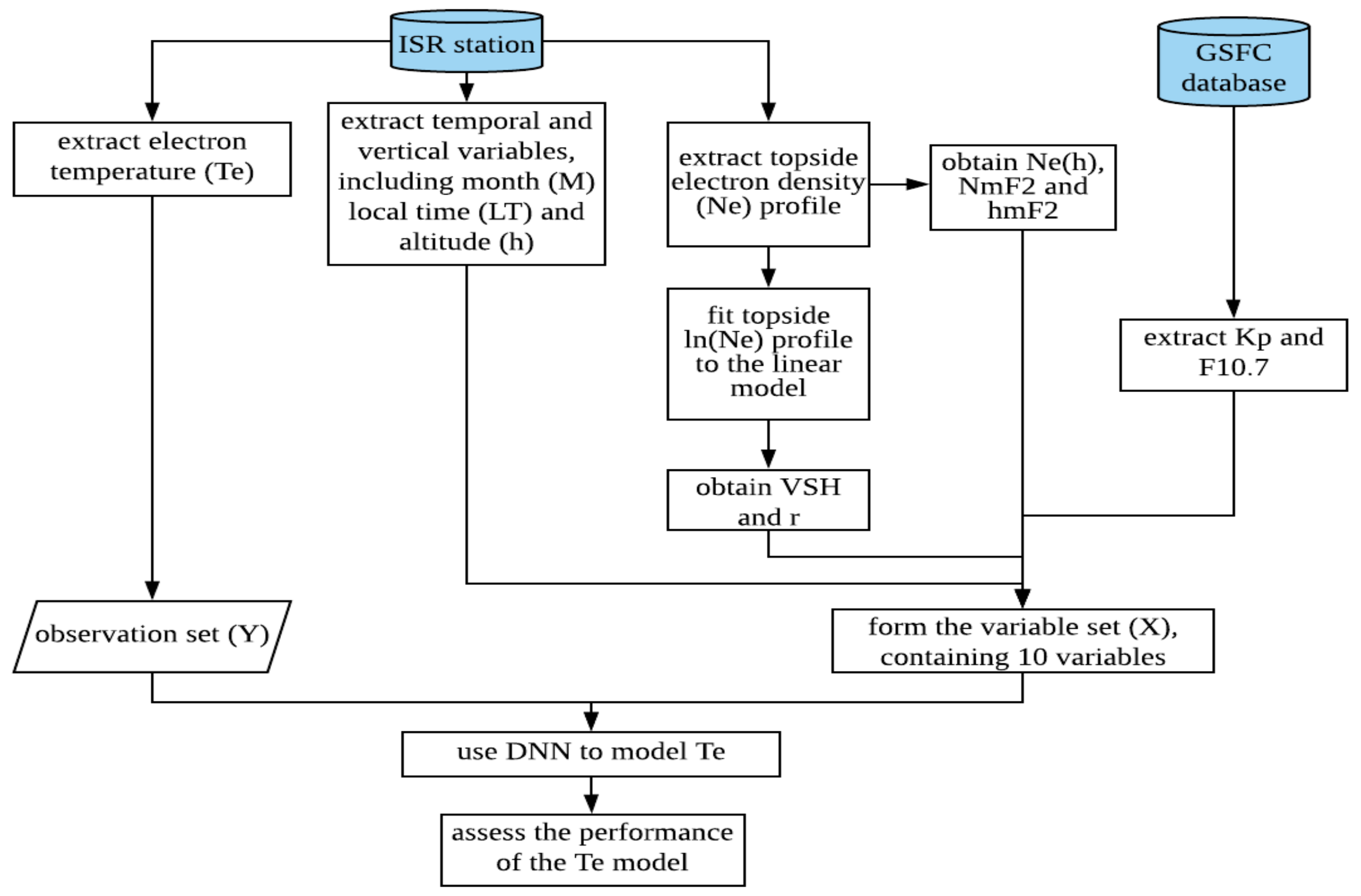

ISR station
GSFC database
extract electron temperature (Te)
extract temporal and vertical variables, including month (M) local time (LT) and altitude (h)
extract topside electron density (Ne) profile
obtain Ne(h), NmF2 and hmF2
fit topside ln(Ne) profile to the linear model
obtain VSH and r
extract Kp and F10.7
observation set (Y)
form the variable set (X), containing 10 variables
use DNN to model Te
assess the performance of the Te model

Fig. 1. Procedure for the application of deep learning to the new Te modeling.

Scheme Number	Variable sets									RMSD (K)
	Height	hmF2	Lat	Kp	[Month, LT]	F10.7	Ne	[VSH, r]	NmF2	
1	1	0	0	0	0	0	0	0	0	612.5
2	1	1	0	0	0	0	0	0	0	510.9
3	1	1	1	0	0	0	0	0	0	485.9
4	1	1	1	1	0	0	0	0	0	402.8
5	1	1	1	1	1	0	0	0	0	368.9
6	1	1	1	1	1	1	0	0	0	323.7
7	1	1	1	1	1	1	1	0	0	304.1
8	1	1	1	1	1	1	1	1	0	294.3
9	1	1	1	1	1	1	1	1	1	291.0

Table 1. Comparison of the RMSDs of Te models obtained from global (Arecibo, Millstone Hill and Poker Flat) measurements and adding candidate variables one-by-one (1 denotes inclusion and 0 denotes non-inclusion).

The full model and outputs can be found at https://gitlab.com/taiyexingshang/electron-temperature-oa

Results

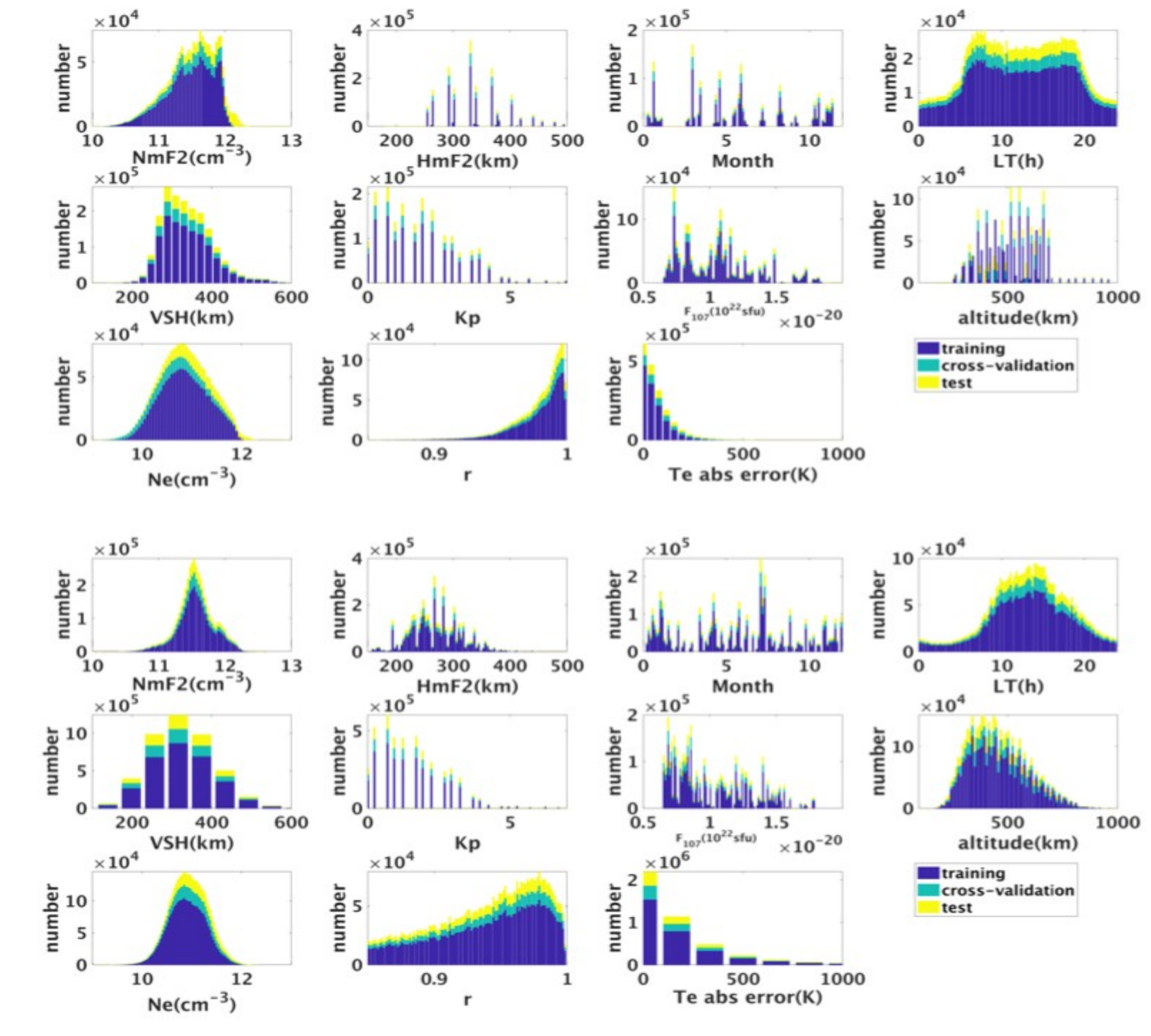

Fig. 2. Distribution of number of ISR observations in each dataset with regards to each variable. Top and bottom figures are for Arecibo and Millstone Hill respectively, during 1970-2013 (actually, Millstone Hill station was fully functional since 1975). The amount of data with regards to Te absolute error is also shown in each panel.

Table 2. RMSD of each Te model (K) in low, middle and high latitude.

Latitude region	DNN(K)	Brace-78(K)	TBT-2012(K)
Low	259	519	413
Middle	254	452	339
High	314	551	455

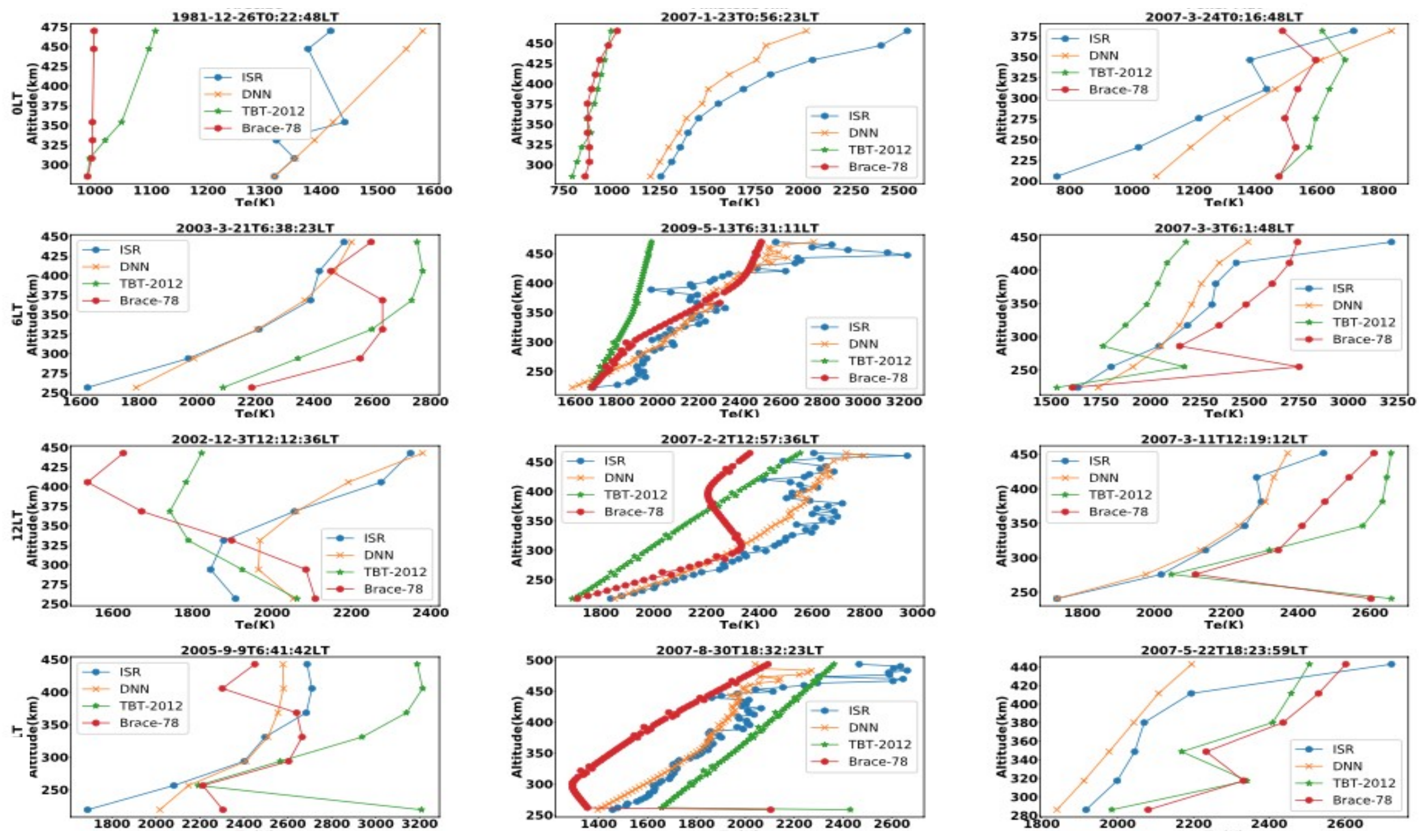

Fig. 3. Four comparison examples of Electron temperature (Te, in degree Kelvin) for the each of three regions based on Arecibo, Millstone Hill and Poker Flat data respectively (which are the left, middle and right figure sets for low, middle, high latitude region respectively), and from top to bottom are examples in 0, 6, 12 and 18 LT respectively. The X and Y axis are Te and height/altitude respectively.

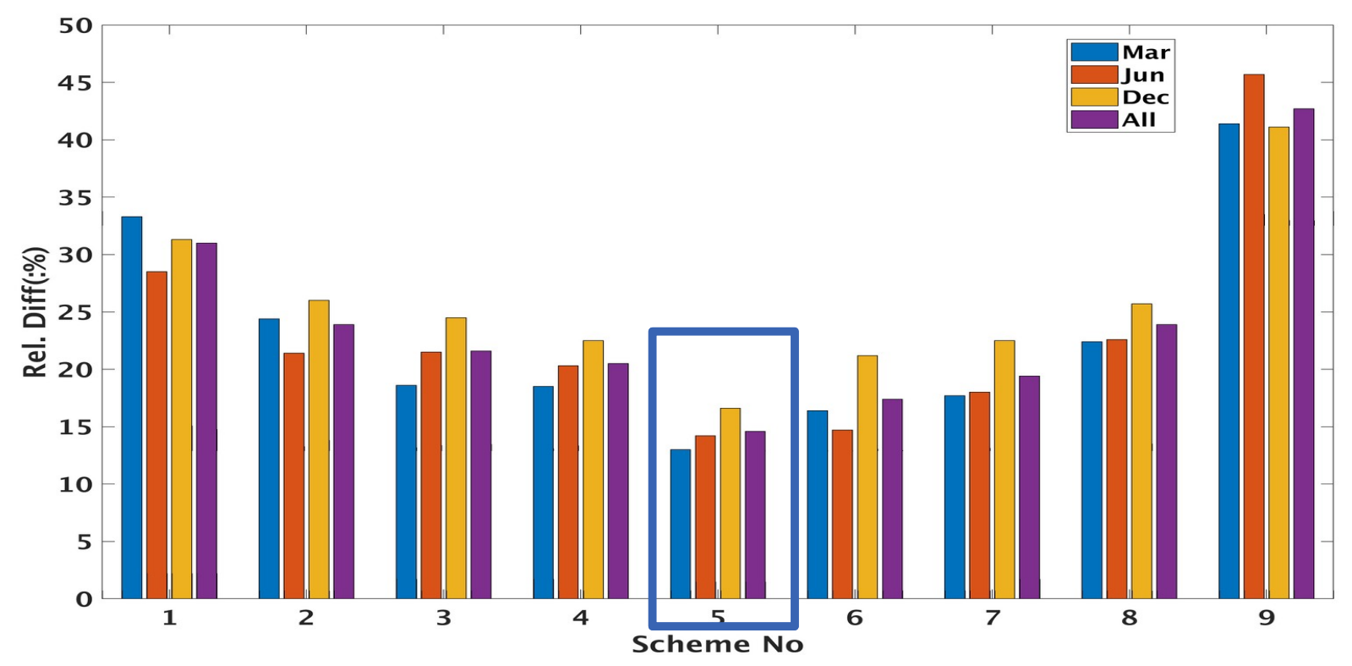

Fig. 4. The weighted RMSD of the relative difference (denoted as Rel.Diff) between the results from the schemes (shown in Table 1) and TIEGCM in three DoIs (March Equinox, June Solstice and December Solstice, 2009, which denote three seasons) and their overall results.

Test Result and Analysis

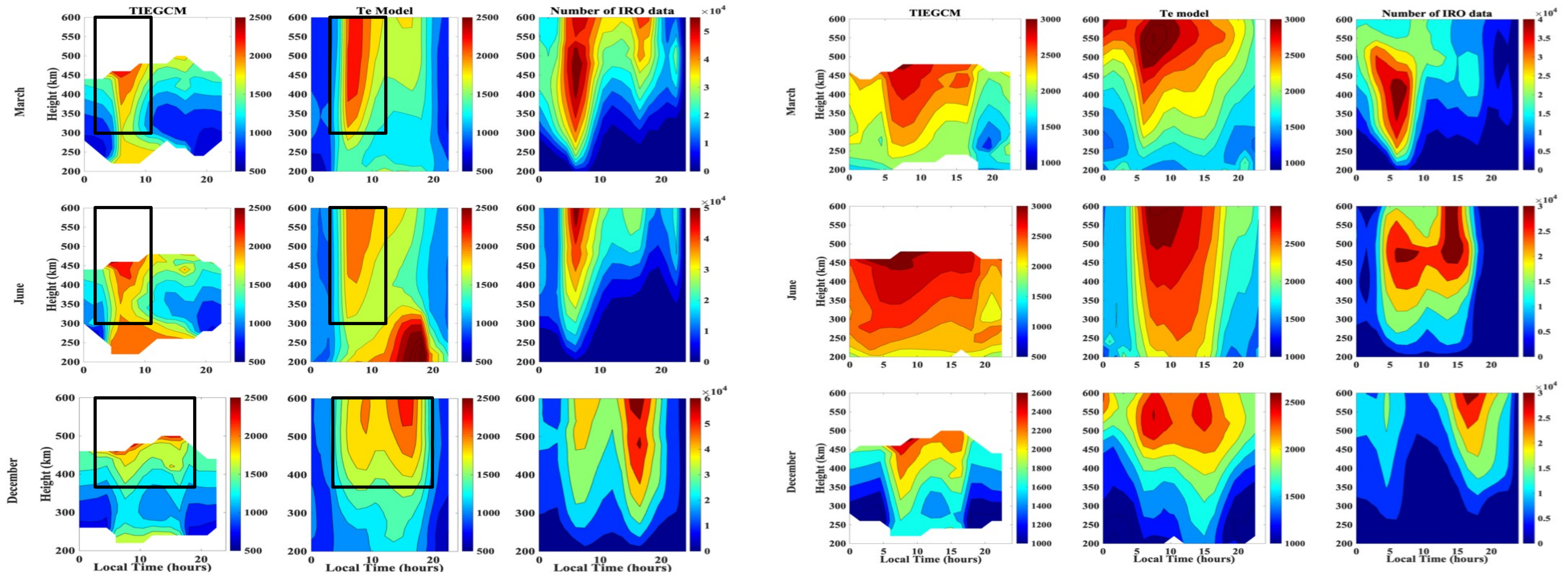

Fig. 5. Electron temperature (Te, in degree Kelvin) obtained from COSMIC data based on Arecibo (left) and Millstone Hill (right) model and those simulated by TIEGCM at solar minimum. The panels from left to right are TIEGCM outputs, predicted mean Te from IRO based on the proposed model and number of available IRO measurements used in each region; from top to bottom are Te for March equinox, June solstice and December, solstice respectively. The X and Y axis are local time and height/altitude respectively.

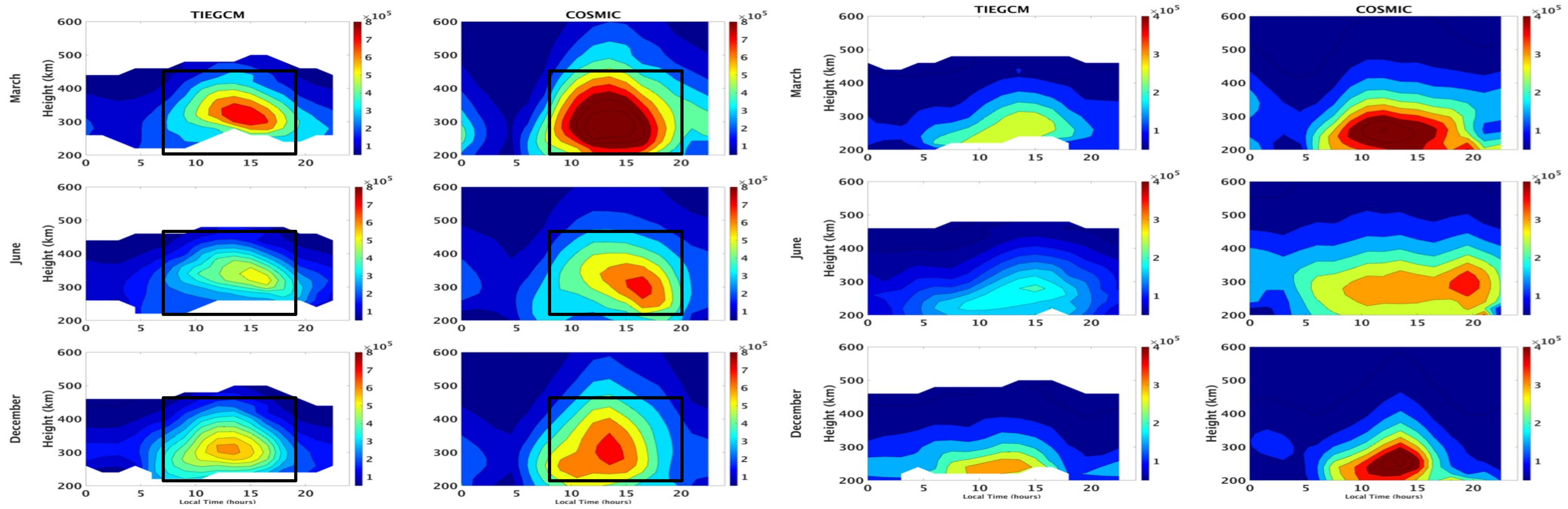

Fig. 6. Electron density (Ne, in el/cm^3) obtained from COSMIC data in low latitudes (left) and mid latitudes (right). Those simulated by TIECHM at solar minimum. The panels from left and right are TIEGCM outputs and mean Ne from COSMIC measurements; from top to bottom are Ne for March equinox, June solstice and December solstice respectively. The X and Y axis are local time and height/altitude respectively.

Conclusion & Future Work

- Te results from the new model were found to **agree more closely than the Brace-78 and TBT-2012 models** with the out-of-sample ISR data from low, mid and high latitudes.
- the characteristics revealed by the **DNN Te results agreed with TIEGCM**, e.g., the clear morning and evening enhancements in the altitude-LT and latitude-LT analysis.
- Furthermore, the study also implies that the bias between the new model and TIEGCM was because **TIEGCM always underestimates the Ne measurements**.

More and more GNSS-IRO satellite missions have been launched (e.g. COSMIC-2, FY-3E, etc), thus the amount of IRO data will increase and the number of Te profiles that can be obtained from our model will increase simultaneously. In conclusion, it is suggested that the proposed Te model could be used to update or improve the current empirical Te models (even for Te modeling in future) and enhance the understanding of the topside ionosphere.

Acknowledgments

This work is supported by the Australian Research Council (ARC) project (LP160100561). This work is also supported by the European Union's Horizon 2020 research and innovation programme under grant agreement No 776262 (AIDA, www.aida-space.eu). We also thank UCAR/CDAAC for providing ionPrf data, OMNIWeb for providing the Kp and F10.7 data and MIT Haystack for providing ISR data..